Hydrol. Earth Syst. Sci. Discuss., 11, 5559–5597, 2014
www.hydrol-earth-syst-sci-discuss.net/11/5559/2014/
doi:10.5194/hessd-11-5559-2014


Hydrology and Earth System Sciences Discussions
Open Access

This discussion paper is/has been under review for the journal Hydrology and Earth System Sciences (HESS). Please refer to the corresponding final paper in HESS if available.

# A pan-African Flood Forecasting System

**V. Thiemig[1,2], B. Bisselink[1], F. Pappenberger[3,4,5], and J. Thielen[1]**

[1]Institute for Environment and Sustainability, Joint Research Centre, Ispra, Italy
[2]Utrecht University, Faculty of Geosciences, Utrecht, The Netherlands
[3]European Centre for Medium-Ranged Weather Forecast (ECMWF), Reading, UK
[4]School of Geographical Sciences, University of Bristol, Bristol, UK
[5]College of Hydrology and Water Resources, Hohai University, Hohai, China

Received: 13 May 2014 – Accepted: 15 May 2014 – Published: 27 May 2014

Correspondence to: V. Thiemig (vera.thiemig@jrc.ec.europa.eu)

Published by Copernicus Publications on behalf of the European Geosciences Union.

## Abstract

The *African Flood Forecasting System* (AFFS) is a probabilistic flood forecast system for medium- to large-scale African river basins, with lead times of up to 15 days. The key components are the hydrological model LISFLOOD, the African GIS database, the meteorological ensemble predictions of the ECMWF and critical hydrological thresholds. In this paper the predictive capability is investigated in a hindcast mode, by reproducing hydrological predictions for the year 2003 where important floods were observed. Results were verified with ground measurements of 36 subcatchments as well as with reports of various flood archives. Results showed that AFFS detected around 70 % of the reported flood events correctly. In particular, the system showed good performance in predicting riverine flood events of long duration (> 1 week) and large affected areas (> 10 000 $km^2$) well in advance, whereas AFFS showed limitations for small-scale and short duration flood events. The case study for "Save flooding" illustrated the good performance of AFFS in forecasting timing and severity of the floods, gave an example of the clear and concise output products, and showed that the system is capable of producing flood warnings even in ungauged river basins. Hence, from a technical perspective, AFFS shows a large potential as an operational pan-African flood forecasting system, although issues related to the practical implication will still need to be investigated.

## 1 Introduction

Riverine floods rank as the second highest death-causing natural disaster in Africa, surpassed only by droughts (Vos et al., 2009). The number of flood-related casualties, affected people, and associated economic losses have significantly increased in Africa since the middle of the 1990s (CRED, 2012), due to an increase of human settlements in flood-prone areas rather than possible climate change issues (Di Baldassarre et al., 2010). Additionally, the fact that most medium- to large-size African river





HESSD
11, 5559–5597, 2014

basins are trans-national is another important influencing factor – (Bakker, 2009) reported that floods occurring in trans-national river basins result in larger losses than if they were occurring in national basins. As a result, flood risk management in Africa has recently gained increased attention in the political and scientific environment (Portuguese Space Office, 2007). Both the Hyogo Framework (United Nations (UN), 2005) and RIO+20 (UNCSD Secretariat, 2012) promote the strengthening of the resilience of African nations to withstand and recover quickly from impacts caused by events of hydro-meteorological origin. The substantial reduction of disaster losses, in lives as well as in social, economic, and environmental assets, is of prime focus. As such, the development of effective early warning systems is fundamental.

An inventory on the "current status on flood forecasting and early warning in Africa" based on reviewing literature, institutional websites and a questionnaire (Thiemig et al., 2011) has revealed a large number of institutional initiatives presently active in flood risk management. An increasing number focus on the development of hydrological forecasting systems. Most of the forecasting endeavours target either short- (< 3 days) or long-range (> 2 weeks) forecasts, but hardly any of them the medium-range (3–15 days). However, medium-range forecasts are crucial for reducing flood-related losses as they provide more time for decision-making and preparation compared to short-range forecasts, as well as more accurate estimations than seasonal forecasts (Thielen et al., 2009a). In particular, probabilistic medium-range flood forecasts based on meteorological EPS, also called HEPS, are of added value as they increase the capability to issue flood warnings earlier and with more confidence than deterministic forecasts, given that they address the associated uncertainties (Cloke and Pappenberger, 2009 and see http://www.hepex.org).

Large research efforts of numerous flood working groups have resulted in an assortment of operational HEPS for various spatial scales (Table 1) (Cloke et al., 2009; Pappenberger et al., 2013). Over the past decade these systems have demonstrated their potential to provide an essential contribution to the prevention and mitigation of flood-related losses, giving additional decision and preparation time prior to a flood





HESSD
11, 5559–5597, 2014

event (Dale et al., 2014; He et al., 2010; Pappenberger et al., 2011; Roulin, 2007). A pan-African HEPS could bridge the gap between the partially existing short and long-ranged flood forecasting systems.

An example of a HEPS operating at continental scale is the European Flood Awareness System (EFAS) (Bartholmes et al., 2009; Pappenberger et al., 2011; De Roo et al., 2011; Thielen et al., 2009b). EFAS uses multiple meteorological weather forecasts, both deterministic (DET) and probabilistic (EPS) (i.e. ECMWF-DET, ECMWF-EPS, German Weather Service-DET and COSMO-LEPS), as input to the hydrological model LISFLOOD (Burek et al., 2013; Van Der Knijff et al., 2010). Using the same model and its parameters for long-term simulations of hydrological conditions in previous decades allows the calculation of flood warning relevant thresholds such as the 5, 10 and 20 year return periods. By applying these thresholds to the forecasts, the ensemble streamflow calculations are converted into effective flood forecasts with up to 10 days lead time. The transferability of the EFAS methods to other climatic regions and flood types has been extensively and successfully tested by Alfieri et al. (2012, 2013) and Thiemig et al. (2010). Additionally, Trambauer et al. (2013) recently confirmed LISFLOOD's suitability as hydrological forecasting model at the pan-African scale, mainly due to its comprehensive representation of the most relevant hydrological processes as well as its applicability as an operational forecasting system with the available data. Therefore, to set up an African flood forecasting system we adopted the methodologies developed for EFAS, and calibrated LISFLOOD for African conditions. The resulting African Flood Forecasting System (AFFS) has the potential to be the first system providing probabilistic medium-ranged hydrological predictions for entire Africa.

The aim of this study is to investigate the predictive capability of AFFS and to estimate its potential as operational flood forecasting system that could in future contribute to the reduction of flood-related losses by providing national and international aid organizations timely with crucial flood forecast information. The predictive capability is assessed in a hindcast mode. For every day of the flood-intense year of 2003, 50 hydrological forecasts are calculated over a lead time of 10 days. Applying hydrological thresholds on the resulting ensemble of hydrological predictions, flood signals can be derived spatially. The forecasting capacity of AFFS is assessed from two perspectives: its overall performance to predict streamflow, and its particular ability to detect and predict flood events. The first is done by calculating the Continuous Rank Probability Score (CRPS), a statistical indicator for probabilistic forecasts, in combination with the limit of predictability, for 36 key locations across Africa to gain an understanding of the general accuracy and the reliable time span of the streamflow forecasts. The second is an event-based analysis, comparing the AFFS flood signals against information collected from various disaster databases such as Dartmouth Flood Observatory, the Emergency Event Database (EM-DAT), the NASA Earth Observatory and Reliefweb to determine the number hits, false alerts and missed alerts as well as the Probability of Detection (POD), False Alarm Rate (FAR) and Critical Success Index (CSI). Lastly, to illustrate the flood forecast performance of AFFS and also to give an example of its potential output, the hindcast for the March 2003 flood event in the Save Basin is presented in detail. The two analyses are complementary in disclosing the strength and shortcomings of AFFS.

The remainder of this article is structured as follows: Sect. 2 gives an outline of the study area and the hydrological reference data used; Sect. 3 describes in detail the structure of AFFS, its functionality as well as the hydrological model LISFLOOD, while Sect. 4 provides details on the setup and verification of the pan-African hindcast. In Sect. 5, results related to LISFLOOD's model performance as well as the forecast capability of AFFS are presented, while Sect. 6 contains a detailed discussion on the results and study limitations, as well as a final conclusion.





HESSD
11, 5559–5597, 2014

## 2 Data

### 2.1 Study area

AFFS forecasting capabilities were tested on the pan-African scale (40° N–35° S; 20° W–60° E). An overview of topographical, meteorological and hydrological conditions, including the delineation of the hydrological basins, altitude and river basin size, time period and length of the wet season, mean annual precipitation, mean annual river discharge, discharge station network and the dominant land use/cover is presented in Fig. 1.

### 2.2 Hydrological reference data

Information about floods, in particular on *when*, *where* and with which *magnitude* a flood event has happened, is required for the optimization of LISFLOOD and the verification of the performance of AFFS. Therefore, discharge observations and information retrieved from various flood archives were employed as hydrological reference data.

#### 2.2.1 Flood archives

Various disaster databases such as the Dartmouth Flood Observatory (Brakenridge, 2013), the Emergency Events Database EM-DAT (CRED, 2012), the NASA Earth Observatory (NASA, 2003) and Reliefweb were used to provide a list of flood events that were reported for Africa in the year 2003. Excluding flash floods, 39 medium- to large-scale flood events were identified. Information on the location and time-period of these events, together with the outline of the affected area, was compiled into a database (see Fig. 2) and used as reference for the event-based verification of the hindcasting performance of AFFS.





HESSD
11, 5559–5597, 2014

### 2.2.2 Discharge observations

Daily discharge records were collected from various national hydrological centres and databases such as the Ethiopian Ministry of Water and Energy, the GLOWA Volta Project, FAO Somalia Water and Land Information Management, the Global Runoff Data Centre (GRDC) and the South African Department of Water Affairs and Forestry (DWAF). The resulting ground observation network comprises 36 discharge measuring stations holding observations between 2003 and 2008 (Fig. 1e). It can be seen that the distribution of stations is not homogeneous, but clustered in certain regions such as Southern Africa, Zambezi and Western Africa.

## 3 African Flood Forecasting System (AFFS)

### 3.1 Structure and functionality

The African Flood Forecasting System (AFFS) aims at producing accurate probabilistic, medium-ranged flood forecast information at the pan-African scale, up to 10–15 days in advance, that could in future support African water authorities timely with valuable information to reduce flood-related losses by increasing preparation time.

A schematic overview, illustrating the structure and functionality of AFFS, is given in Fig. 3.

For the calculation of flood forecasts, AFFS requires a hydrological model, four main data sources, as well as four main processes. The model selected for AFFS is the physically-based hydrological model LISFLOOD and is described in detail in Sect. 3.2. The five main data sources on which AFFS relies are: historical hydrological observations, historical as well as near real-time meteorological observations, real-time meteorological forecasts and an African GIS dataset. Specifications of these are given in Sect. 4.1. The four main processes AFFS runs are: the calculation of hydrological thresholds, the computation of the initial hydrological conditions, the computation of the ensemble hydrological predictions, and the identification of flood events. Each is described in detail in the following:

1. *The calculation of hydrological thresholds.* Hydrological thresholds facilitate the distinction between flood and no-flood situations, as well as the distinction between various flood magnitudes, when applied on the hydrological EPS predictions (step 3). The hydrological thresholds used within AFFS are the 2, 5, 10 and 30 year return periods, corresponding to low, medium, high and severe flood events respectively. These are derived for each 0.1° pixel based on a long-term discharge simulation, resulting from forcing LISFLOOD with the African GIS dataset and daily historical meteorological data (here over 21 years; 1989–2010).

2. *The computation of the initial hydrological conditions.* Information about the current hydrological conditions, meaning all state variables of the water cycle, is required for each day during the forecasting period to initialize LISFLOOD prior to calculating hydrological predictions (step 3). State variables are calculated for each 0.1° pixel by forcing LISFLOOD with the near real-time meteorological observations over the forecasting period (here: 1 January–31 December 2003).

3. *The computation of the ensemble hydrological predictions.* Hydrological predictions (with 10 days lead time) are calculated by running LISFLOOD for each forecasting date with the respective initial hydrological conditions (step 2) and the probabilistic real-time weather forecasts.

4. *The identification of flood events.* The flood forecast itself results from comparing the ensemble of hydrological predictions (step 3) against the hydrological thresholds (step 1). A flood signal is identified if all of the following conditions are satisfied. First, that at least 30 or 15 out of the 50 hydrological predictions exceed the threshold of 2 or 10 year return period respectively for at least three consecutive days. Second, that the upstream area is larger than 15 000 $km^2$, and third, that more than 10 clustered river pixels are affected.





HESSD
11, 5559–5597, 2014

The results are visualized in so-called “threshold exceedance maps”, as well as ensemble quantile plots at key locations.

### 3.2 Hydrological framework

LISFLOOD is a fully-distributed, physically-based hydrological model (Burek et al., 2013; Van Der Knijff et al., 2010) that simulates the spatial and temporal pattern of catchment responses in medium- to large-scale river basins as a function of spatial information about meteorology, topography, soil and land cover. Originally, LISFLOOD was developed specifically to simulate hydrological processes in large river basins, and later optimized for flood forecasting on the European Scale within the framework of the European Flood Awareness System (www.efas.eu) (Bartholmes et al., 2009; Pappenberger et al., 2011; Ramos et al., 2007; De Roo et al., 2011; Thielen et al., 2009b). Since then the range of application has been extended successfully to studies dealing with climate change impact assessment (Dankers and Feyen, 2008, 2009; Feyen et al., 2009; Rojas et al., 2012), flash flood forecasting (Alfieri et al., 2012) and water resources (Mubareka et al., 2013; Sepulcre-Canto et al., 2012). For a full description on the model structure and equations the reader is referred to Burek et al. (2013).

For AFFS, LISFLOOD was set up on the pan-African scale with a spatial resolution of 0.1°. The model structure was extended to also account for large reservoirs as well as for transmission loss along the river channel, which is very significant in large river systems in semi-arid areas (Haddeland et al., 2011). All GIS-based model parameters were either extracted or derived from the African GIS dataset. The African GIS dataset comprises a collection of thematic layers providing information on topography, river channel geometry, land use, soil and vegetation properties, extracted from different data sources such as the Harmonized World Soil Database 1.0, the VGT4AFRICA project or the SRTM. A more detailed description of the input maps for Africa is given by Bodis (2009).

In the current setup, layers of water use information from the Global Crop Water Model (GCWM) (Siebert and Döll, 2008, 2010) are dynamically coupled with





HESSD
11, 5559–5597, 2014

LISFLOOD. It is assumed that water is subtracted solely from the river discharge, not from internal storages.

The local drain direction network (LDD) of the African river basins is developed using a sequence of upscaling operations performed on the flow network, derived from a high-resolution Shuttle Radar Topography Mission (SRTM)-based elevation model of Africa. By upscaling from a fine to a coarser scale, the accuracy of the hydrography data can be lost and manual corrections should be applied. In the current pan-African setup we applied the new algorithm for automatic upscaling of river networks successfully developed by Wu et al. (2011) that address many of these upscaling issues.

Meteorological variables were obtained from the ERA-Interim and ECMWF-EPS fields (Simmons et al., 2007). Parameters related to groundwater response, infiltration, groundwater losses, channel routing and reservoir operating rules were determined through model calibration.

The pan-African set-up was calibrated for 36 sub-catchments (see green dots in Fig. 1e), corresponding to 11 hydrological basins, over a time period of five years (2004–2008; 2003 used as warm-up). Balsamo et al. (2010) and Di Giuseppe et al. (2013) reported on systematic biases in the ERA-Interim precipitation data. To correct for these biases, we have used the ERA-Interim precipitation which was corrected using the Global Precipitation Climatology Project (GPCP) dataset from the European Centre for Medium-range Weather Forecasts (ECMWF). Details of the rescaling method can be found in Balsamo et al. (2010). The calibration was done using a state-of-the-art Particle Swarm Optimisation (PSO) algorithm particularly designed for hydrological applications, called hydroPSO (Zambrano-Bigiarini and Rojas, 2012, 2013), which has recently been applied successfully for the optimization of LISFLOOD over various African river basins (Thiemig et al., 2013). The selection of model parameters to be calibrated is listed in Table 2, including their respective physically-reasonable ranges. The performance of each calibration iteration was assessed using the modified Kling-Gupta Efficiency (KGE') (Kling et al., 2012).





HESSD
11, 5559–5597, 2014

The KGE' is a recent performance indicator based on the equal weighting of linear correlation ($r$), bias ratio ($\beta$) and variability ($\gamma$), between simulated (s) and observed (o) discharge:

$$\mathrm{KGE}' = 1 - \sqrt{(r-1)^2 + (\beta-1)^2 + (\gamma-1)^2} \tag{1a}$$

$$\beta = \frac{\mu_\mathrm{s}}{\mu_\mathrm{o}} \tag{1b}$$

$$\gamma = \frac{\mathrm{CV}_\mathrm{s}}{\mathrm{CV}_\mathrm{o}} = \frac{\sigma_\mathrm{s}/\mu_\mathrm{s}}{\sigma_\mathrm{o}/\mu_\mathrm{o}} \tag{1c}$$

where $r$ is the Pearson product-moment correlation coefficient, $\mu$ is the mean discharge [$\mathrm{m^3\,s^{-1}}$], CV is the coefficient of variation and $\sigma$ is the standard deviation of the discharge [$\mathrm{m^3\,s^{-1}}$]. KGE', $r$, $\beta$ and $\gamma$ are dimensionless and their optimum is at unity. The value of KGE' gives the lower value of any of the three sub-components ($r$, $\beta$ and $\gamma$). The hydrological performance can be classified using KGE' as following (Kling, 2012):

- good (KGE' $\geq$ 0.75),
- intermediate (0.75 > KGE' $\geq$ 0.5),
- poor (0.5 > KGE' > 0.0) and
- very poor (KGE' $\leq$ 0.0).

The benefits of using KGE' over KGE or Nash–Sutcliff Efficiency are discussed by Gupta et al. (2009) and demonstrated by Thiemig et al. (2013).

## 4 Pan-African hindcast for 2003

The potential of AFFS as a future pan-African flood forecasting system for medium- to large-scale river basins and the medium-range (with up to 10 i.e. 15 days lead time)





HESSD
11, 5559–5597, 2014

is tested in a retrospective analysis in which hydrological predictions are calculated over a certain time period in the past for which the true hydrological situation is already known, i.e. so-called hindcasts. Comparing the results of the hindcasts against available information on the true hydrological situation provides the opportunity to assess the predictive capabilities of AFFS. A pan-African hindcast was therefore computed for the whole year of 2003.

### 4.1 Set-up

The hindcast was computed with AFFS using the calibrated LISFLOOD setting (Sect. 3.2) and following the workflow as described in Sect. 3.1.

The hydrological thresholds (2 and 10 year return periods) were derived for each 0.1° pixel from a long-term discharge simulation resulting from forcing LISFLOOD with daily GPCP-corrected ERA-Interim data over a time period of 21 years (1989–2010). The initial hydrological conditions, i.e. all state variables, were computed for each forecasting date between 1 January and 31 December 2003 by running LISFLOOD with near real-time meteorological observations. During the hindcasting period these needed to be approximated by using the daily GPCP-corrected ERA-Interim; however, during real-time forecasting, the first day of each ECMWF deterministic forecast could be used. The ensemble of hydrological predictions was computed by forcing LISFLOOD for each forecasting date with the previously determined daily initial conditions and the respective real-time meteorological forecast. Here, we employed the 10-day probabilistic ECMWF-ENS (Buizza et al., 2007, 2008; Leutbecher and Palmer, 2008) as the real-time meteorological forecast, since the 15 day ECMWF-ENS (Buizza et al., 2007) was only available after March 2003. Flood events were identified by comparing the ensemble of hydrological predictions against the critical thresholds.





HESSD
11, 5559–5597, 2014

### 4.2 Verification

The capability of AFFS to predict streamflow in general, and flood events in particular, is assessed by comparing the hindcasting results with available ground observations and information from disaster databases respectively, using various evaluation methods presented in detail in the following.

#### 4.2.1 General streamflow

The performance in predicting streamflow is evaluated based on the Continuous Rank Probability Skill Score (CRPSS). The CRPSS is calculated by dividing the CRPS (Continuous Rank Probability Score), which compares the cumulative distribution function of a probabilistic forecast ($P^{\text{hydEPS}}$), to the observation ($P^{\text{obs}}$), through a benchmark as follows:

$$\text{CRPS} = \frac{1}{n}\sum_{i=1}^{n}\int_{x=-\infty}^{x=\infty}\left(P_i^{\text{hydEPS}}(x) - P_i^{\text{obs}}(x)\right)^2 d \tag{2}$$

$$\text{CRPSS} = 1 - \frac{\text{CRPS}_{\text{forecast}}}{\text{CRPS}_{\text{benchmark}}} \tag{3}$$

using the *Heaviside Function* (Hersbach, 2000). Values range from minus infinity to one, where one represents the optimum, and negative values indicate a non-skilful forecast.

The range of days in which the forecast is skilful is expressed by the *limit of predictability*. The limit of predictability determines the number of days before the ensemble of hydrological forecasts deviates on average more from the actual observation than the long-term mean. This gives the limiting point until which the forecasts have added value compared to the long-term mean. Mathematically it coincides with the CRPSS being equal to zero.





HESSD
11, 5559–5597, 2014

In this study, the CRPSS was calculated for each lead time at the 36 key locations all over Africa. For the calculation of the CRPS, discharges were normalized to remove possible systematic biases, while the seasonal mean was used as benchmark. The CRPSS for the lead-times of 3, 5 and 8 days is presented together with the limit of predictability in Sect. 5.2.1 facilitating the evaluation of AFFS' general ability to predict streamflow.

### 4.2.2 Flood events

The ability of AFFS to detect flood events is assessed using a contingency table in combination with several skill scores such as the Probability of Detection (POD), the False Alarm Rate (FAR) and the Critical Success Index (CSI), that can be derived based upon this table.

The contingency table is a performance measure summarizing all possible forecast-observation combinations such as hits (H; event forecasted and observed), misses (M; event observed but not forecasted), false alarms (FA; event forecasted but not observed) and correct negatives (CN; event neither forecasted nor observed) (see Table 3). The POD, FAR and CSI provide further measures to quantify the ability of AFFS to identify flood events by providing success and failure rates. The POD and CSI give the proportion between successfully forecasted flood events and all observed flood events i.e. the total number of observed and forecasted flood events, respectively; while the FAR gives the proportion of falsely forecasted flood events considering all forecasted flood events. All are expressed as percentages.

$$\mathrm{POD} = \frac{\mathrm{H}}{\mathrm{H}+\mathrm{M}} \cdot 100 \tag{4}$$

$$\mathrm{CSI} = \frac{\mathrm{H}}{\mathrm{H}+\mathrm{FA}+\mathrm{M}} \cdot 100 \tag{5}$$

$$\mathrm{FAR} = \frac{\mathrm{FA}}{\mathrm{H}+\mathrm{FA}} \cdot 100 \tag{6}$$





HESSD
11, 5559–5597, 2014

The optimum value for POD and CSI is at 100 %; whereas it is 0 % for FAR.

Information regarding observed flood events was retrieved from several disaster databases (Fig. 2), while forecasted flood events were identified by inspecting the threshold exceedance maps. Based on these maps, a hydrological situation was classified as a flood event if least 30 or 15 members exceed respectively the 2 or 10 year return period threshold persistently for at least 3 consecutive days, in a catchment with an upstream area of 15 000 $km^2$ or more. 40 flood events were forecasted for the year 2003; information regarding time period and location was compiled in (Fig. 4).

## 5 Results

### 5.1 Model performance

Figure 5 presents the model performance of LISFLOOD during the calibration period (2004–2008) for the 36 catchments in terms of KGE'. 31 out of 36 catchments (86 %) have a KGE' greater than 0.5, and 50 % are greater than 0.75, indicating very good hydrological performances for most catchments. Poorer hydrological performances (KGE' $< 0.5$) are clustered in smaller tributaries in the arid area of South Africa and in a station in the Niger River, where the observation records are questionable.

The hydrological performance during the validation period (1998–2003) is illustrated in Fig. 6. It shows the KGE' for only 34 catchments, as there were no observations available for the remaining two stations for this specific time period. More than half of the KGE' values are greater than 0.5, and 29 % are greater than 0.7. The difference in KGE' between the calibration and the validation period is largest in the Zambezi catchment due to a lack of data in the calibration period as for instance seen in Fig. 7.

Figure 7 shows the comparison between simulated and observed hydrographs for four selective locations in Africa (see Fig. 1e). For the Niger River (Fig. 7a) it can be seen that the flow dynamics are well reproduced during both calibration and validation, while the flow volume is only well captured during calibration, and slightly worse during





HESSD
11, 5559–5597, 2014

validation, where it shows an underestimation. One reason for this could be related to the length of the calibration period for this catchment, which might be too short to determine the optimum value for the calibration parameters. Also in the Kafue River (Fig. 7b) the parameter optimization is only based on a 2 year period. However, the discharge is reproduced well during both calibration and validation, with the exception of the year 2001, in which the discharge is largely overestimated, resulting into a decreased KGE' of 0.36 during validation. For the Olifants River (Fig. 7c) the tendencies during both calibration and validation are similar, showing a fairly well captured flood dynamic with some extreme overestimations in flood volume resulting into a KGE' of 0.34 (calibration) and 0.56 (validation). For the Juba River (Fig. 7d), the KGE' indicates a satisfactory reproduction of discharges during calibration, but not during validation in which the KGE' is negative. This is due to the combination of the extreme overestimation in the year of 2003 and the short length of validation period.

## 5.2 Forecast verification

### 5.2.1 Streamflow

The overall performance of the forecast is analysed by comparing the hydrological forecasts against ground observations using the CRPSS and the limit of predictability. In Fig. 7 the CRPSS is plotted over the 10 days lead time. The average CRPSS ranges between 0.4 and 0.5, showing a steadily decreasing tendency after Day 3 (the red graph in Fig. 7a), meaning that the error increases, i.e. AFFS' skill to forecast streamflow decreases. This is also confirmed by the number of stations with positive CRPSS, which continuously decreases over the 10 days lead time from 65 to 45 % (the red graph in Fig. 7b). Decomposing the CRPSS for different regions in Africa shows that only a small number of stations in Eastern Africa (20 %) have skilful streamflow predictions, but the opposite is true for Western Africa (70–90 %). The decomposition of the CRPSS for different ranges of average annual precipitation amounts indicates that the predictability of streamflow is generally slightly lower in arid areas (average amount of annual precipitation < 600 mm). Figure 8 compares the forecast to a seasonal benchmark and indicates the number of days the forecast is skilful – this is also called the limit of predictability. A few stations indicate that a skilful forecast can be achieved up to Day 10, and that at some stations no skilful predictions have been made for this year in comparison to the long-term mean. Whether the decrease in forecasting performance is caused by possibly inaccurate ENS cannot be assessed here, as the influence of the ENS cannot be filtered out. However, cross-comparing the CRPSS and the limit of predictability with the KGE' received during calibration (Fig. 4) suggests that the skill of AFFS to predict streamflow is strongly dependent on the optimization of the hydrological model. For locations where LISFLOOD seems to be well fitted, expressed by a good hydrological performance (KGE' > 0.6), the forecasts were mostly skilful (positive CRPSS); while they were without skill (CRPSS negative and limit of predictability equal zero) exclusively at locations where the KGE' was less than 0.6 during calibration. Regarding catchments, AFFS showed to have particular skill at predicting streamflow for the Volta, Baro-Akobo, Kunene and the Upper Zambezi river basins.

### 5.2.2 Flood events

Table 4 summarizes AFFS's ability to identify flood events. In general, comparing the 39 reported flood events (Fig. 2) with the 40 forecasted ones (Fig. 4), 27 of the reported events were forecasted correctly by AFFS, while 12 were missed and 11 events that were forecasted were not reported; resulting into a general POD of 69 %, a FAR of 29 % and a CSI of 54 %.

In order to gain a clearer understanding of what might be influencing factors that determine the strengths and limitations of AFSS to identify flood events, the analysis was repeated for different flood durations (more or less than a week), climatic conditions (more or less than 600 mm average annual precipitation) as well as for different estimated sizes and average annual discharges of the affected area (more or less than 10 000 $km^2$; and more or less than 10 $km^2\,year^{-1}$); and lastly also for different African regions (Northern, Western, Eastern and Southern Africa) as it might be of particular





HESSD
11, 5559–5597, 2014

interest to potential future users of AFFS (see Table 4). The analysis shows that the probability of AFFS detecting a flood event seems to be particularly high for floods whose affected area is large (> 10 000 km$^2$), the flood duration long (> 1 week) and the amount of annual precipitation not very high (≤ 600 mm a$^{-1}$); whereas the probability of missing a flood event is notably higher if the flood is of short duration (≤ 1 week) or the affected area relatively small (≤ 10 000 km$^2$). The False Alarm Rate indicates that AFFS predicts more flood events in regions with less than 10 km$^2$ mean annual discharge as well as flood events with large affected areas. However, it is unjustified to claim with certainty that these flood events were falsely predicted as there is also the possibility that they were just not reported. Finally, the Critical Success Index is quite similar for all the different categories, ranging from 46 to 65 %. Comparing the performance for the different regions, the high POD for Eastern Africa as well as the low FAR of Western Africa are the most distinct, while the performances in the other regions are quite similar. In summary, AFFS holds in general a good ability to forecast the occurrence of flood events as the POD is always much higher than the FAR, and the CSI is generally above 50 %.

Figure 9 presents the flood forecast for the March 2003 event in the Save Basin (for location see Fig 1) as a visual example of a flood forecast obtained with AFFS. Note that there were no ground observations available to optimize LISFLOOD for this basin; hence the model was run with the default parameterization. The threshold exceedance maps (Fig. 9a) show the number of hydrological ensembles exceeding a certain critical threshold for a specific calendar date and lead time. Here the 2 year return period is chosen as the critical threshold. Forecasts are shown for the 3, 5, 7, 9 and 12 March with lead times of 3, 5 and 8 days. Additionally, ensemble quantile plots (Fig. 9b) illustrate the 10 day probabilistic hydrological prediction for a specific location, including various specific EPS ranges (median, 1st and 3rd quartile) and critical hydrological thresholds (2, 5, 10 and 30 year return periods corresponding to low, medium, high and severe flooding respectively). Here, the 10 day forecasts obtained on the 2 and 3 March for one specific reporting point are shown (for the location see





HESSD
11, 5559–5597, 2014

the red star in the upper left panel of Fig. 9a). Based on those AFFS output products, the onset of the flood event is forecasted with a lead time of 8 days for the 5 March, which coincides perfectly with information given by the Dartmouth Flood Observatory who reported flooding in the Save and tributaries between the 5 and 16 March 2003 (Fig. 2, obsID10). At the reporting point, the flood magnitude was forecasted (according to the EPS median) to exceed the 10 year return period, which also agrees with the severity classification of the observed flood event as given by the Dartmouth Flood Observatory: "Class 1: large flood events: significant damage to structures or agriculture; fatalities; and/or 1–2 decades-long reported interval since the last similar event". This example demonstrates that although there are no ground observations available for this basin, AFFS is capable of producing timely and accurate flood forecasts. Although this is only a single case study, the results show clearly that AFFS has the potential to support national and international organisations in future to prevent and/or mitigate flood-related damages and losses.

## 6 Discussion and conclusion

The predictive capability of the African Flood Forecasting System (AFFS) was investigated in a hindcast mode to estimate its potential as an operational flood forecasting system for the whole of Africa.

AFFS detected correctly the majority of reported flood events. The system showed particular strength in predicting riverine flood events of long duration (>1 week) and large affected areas ($>10\,000\,\mathrm{km}^2$). This type of flood has the capacity to impact the socio-economic structures of a country to the extent that it might cause setbacks in the country's development (UNCSD Secretariat, 2012; United Nations (UN), 2005). The example of the flood forecast for the Save River demonstrated the precision of AFFS, gave an example of the output products that could provide the end-user with clear and concise information about the possible future hydrological situation, and showed that AFFS is capable of producing flood warnings even in ungauged river basins, i.e. in river





HESSD
11, 5559–5597, 2014

basins where no observations are in the public domain. Hence, AFFS demonstrated a good potential to predict large-scale and long duration flood events well in advance.

On the other hand, one might raise concern about the FAR, which suggest that 29 % of all flood events that AFFS predicted did not happen. However, first of all, the fact that these floods were not reported in one of the disaster databases does not necessarily mean that they did not actually happen, as there is no certainty that every flood that occurred was also reported, hence the database of observed events (Fig. 2) might be not complete. Second, AFFS is a probabilistic flood forecasting system and as such it gives the probability with which a flood event might happen; i.e. a flood that is predicted with a probability of 70 % should (ideally) also occur in only 70 % of cases and not in all. Hence, the user has to keep in mind the difference between a deterministic and probabilistic forecast while interpreting the results.

The limitations of AFFS center around the detection of flood events with short durations (< week) and/or small affected areas ($\leq 10\,000\,\text{km}^2$), as well as for flood events occurring close to the boundaries of the Intertropical Convergence Zone. The difficulties in detecting relatively small and/or short duration flood events is most likely due to the combination of a) the limited precision given by SRFE to capture small-scale meteorological events accurately in the correct time and place, and b) the relatively coarse grid size of $0.1 \times 0.1°$ that AFFS is operating on, which might be too coarse for these type of floods. For flood events occurring closely at the boundaries of the ITCZ the forecasts may suffer from a displacement of the ITCZ controlling the onset and spatial extent of the West-Africa Monsoon, a conclusion also reached by Di Giuseppe et al. (2013).

This study has illustrated the structure and workflow of AFFS and a first evaluation upon its performance. The results indicate that system improvements and more detailed calibration of the system are needed. However, despite the limitations of the current setup, the system detected the majority of reported floods correctly even though LISFLOOD has been optimized using only a relatively small number of hydrological records (36 over the whole of Africa). This shows that the system works well with a





HESSD
11, 5559–5597, 2014

minimum number of ground observations, while at the same time, it indicates a good potential for further improvements once more observational records become available. Furthermore, in areas where the limit of predictability is currently at 10 days the potential lead-time could easily be extended up to 15 days by using the ECMWF-ENS which are available for the time period after March 2003. Additionally, a cross-comparison study of AFFS with other global forecasting or nowcasting systems is necessary to gain a deeper understanding on the particular strengths and limitations of AFFS, as well as to examine issues such as whether there is a necessity for a hydrological model, or the detail of output products required to be useful for the end-users. This will therefore be the focus of future research. The HEPEX initiative (www.hepex.org) and the recently-launched Global Flood Partnership http://portal.gdacs.org/Global-Flood-Partnership) will be explored as a possibility for further testing of AFFS in research and experimental real-time mode. Lastly, this study only evaluated the technical feasibility of AFFS, while issues related to practical implications such as potential implementing institutes, funding and availability of technical expertise were beyond the remit of this study, but would be highly relevant to future research.

Concluding upon AFFS, this study has demonstrated that this system has a great potential to contribute to the reduction of flood-related losses in Africa by providing national and international aid organizations timely with crucial flood forecast information.

*Acknowledgements.* The Ethiopian Ministry of Water and Energy, the GLOWA Volta Project, FAO Somalia Water and Land Information Management, the Global Runoff Data Centre and the South African Department of Water Affairs and Forestry provided us kindly with hydrological ground measurements. Flood reports were obtained from the Dartmouth Flood Observatory, the Emergency Events Database EM-DAT, the NASA Earth Observatory and the Reliefweb. We also acknowledge sincerely Ad de Roo and Steven De Jong for PhD supervision; Peter Burek and Alessandra Bianchi for providing technical assistance; and William Edward Becker for proofreading.





HESSD
11, 5559–5597, 2014

## References

Alfieri, L., Thielen, J., and Pappenberger, F.: Ensemble hydro-meteorological simulation for flash flood early detection in southern Switzerland, J. Hydrol., 424–425, 143–153, 2012.

Alfieri, L., Burek, P., Dutra, E., Krzeminski, B., Muraro, D., Thielen, J., and Pappenberger, F.: GloFAS – global ensemble streamflow forecasting and flood early warning, Hydrol. Earth Syst. Sci., 17, 1161–1175, doi:10.5194/hess-17-1161-2013, 2013.

Arheimer, B., Lindström, G., and Olsson, J.: A systematic review of sensitivities in the Swedish flood-forecasting system, Atmos. Res., 100, 275–284, 2011.

Bakker, M. H. N.: Transboundary river floods: examining countries, international river basins and continents, Water Pol., 11, 269–288, 2009.

Balsamo, G., Boussetta, S., Lopez, P., and Ferranti, L.: Evaluation of ERA-Interim and ERA-Interim-GPCP-rescaled Precipitation Over the U.S.A. (European Centre for Medium Range Weather Forecasts), Shinfield Park, Reading, Berkshire, UK, ERA report series, no. 5, 2010.

Bartholmes, J. C., Thielen, J., Ramos, M. H., and Gentilini, S.: The european flood alert system EFAS –Part 2: Statistical skill assessment of probabilistic and deterministic operational forecasts, Hydrol. Earth Syst. Sci., 13, 141–153, doi:10.5194/hess-13-141-2009, 2009.

Bodis, K.: Development of a data set for continental hydrologic modelling Input layers related to topography, channel geometry, land cover and soil characteristics of European and African river basins, Office for Official Publications of the European Communities, Luxembourg, 80 pp., doi:10.2788/46925, 2009.

Brakenridge, G. R.: Global Active Archive of Large Flood Events, Dartmouth Flood Observatory, University of Colorado, available at: http://floodobservatory.colorado.edu/Archives/index.html, 2013.

Buizza, R., Bidlot, J. R., Wedi, N., Fuentes, M., Hamrud, M., Holt, G., and Vitart, F.: The new ECMWF VAREPS (Variable Resolution Ensemble Prediction System), Q. J. Roy. Meteorol. Soc., 133, 681–695, 2007.

Buizza, R., Leutbecher, M., and Isaksen, L.: Potential use of an ensemble of analyses in the ECMWF Ensemble Prediction System, Q. J. Roy. Meteorol. Soc., 134, 2051–2066, 2008.

Burek, P., Van Der Knijff, J., and De Roo, A.: LISFLOOD, distributed water balance and flood simulation model – Revised user manual 2013 (Ispra: Institute for Environment and Sustainability), 2013.





HESSD
11, 5559–5597, 2014

A pan-african flood forecasting system

V. Thiemig et al.

Cloke, H. L. and Pappenberger, F.: Ensemble flood forecasting: A review, J. Hydrol., 375, 613–626, 2009.
Cloke, H., Thielen-del Pozo, J., Pappenberger, F., Nobert, S., Balint, G., Edlund, C., Koistinen, A., De Saint Aubin, C., Sprokkereef, E., Viel, C., Salamon, P., and Buizza, R.: Progress in the Implementation of Hydrological Ensemble Prediction Systems (HEPS) in Europe for Operational Flood Forecasting, EcMWF Newsl., 121, 21–25, 2009.
CRED, C. for R. on the E. of D.: The OFDA/CRED International Disaster Database, available at: www.emdat.be, 2012.
Dale, M., Wicks, J., Mylne, K., Pappenberger, F., Laeger, S., and Taylor, S.: Probabilistic flood forecasting and decision-making: an innovative risk-based approach, Nat. Hazards, 70, 159–172, 2014.
Dankers, R. and Feyen, L.: Climate change impact on flood hazard in Europe: An assessment based on high-resolution climate simulations, J. Geophys. Res. Atmos., 113, D19105, doi:10.1029/2007JD009719, 2008.
Dankers, R. and Feyen, L.: Flood hazard in Europe in an ensemble of regional climate scenarios, J. Geophys. Res. Atmos., 114, D16108, doi:10.1029/2008JD011523, 2009.
De Roo, A., Thielen, J., Salamon, P., Bogner, K., Nobert, S., Cloke, H., Demeritt, D., Younis, J., Kalas, M., Bódis, K., Muraro, D., and Pappenberger, F.: Quality control, validation and user feedback of the European Flood Alert System (EFAS). Int. J. Digit. Earth, 4, 77–90, 2011.
Di Baldassarre, G., Montanari, A., Lins, H., Koutsoyiannis, D., Brandimarte, L., and Blöschl, G.: Flood fatalities in Africa: From diagnosis to mitigation, Geophys. Res. Lett., 37, L22402, doi:10.1029/2010GL045467, 2010.
Feyen, J., Shannon, K., and Neville, M.: Proceedings of The International Urban Water Conference, Heverlee, Belgium, 15–19 September, 2008: Water and Urban Development Paradigms Towards an Integration of Engineering, Design and Management Approaches, 2009.
Di Giuseppe, F., Molteni, F., and Dutra, E.: Real-time correction of ERA-Interim monthly rainfall, Geophys. Res. Lett., 40, 3750–3755, 2013.
Gupta, H. V., Kling, H., Yilmaz, K. K., and Martinez, G. F.: Decomposition of the mean squared error and NSE performance criteria: Implications for improving hydrological modelling, J. Hydrol., 377, 80–91, 2009.
Haddeland, I., Clark, D. B., Franssen, W., Ludwig, F., Voß, F., Arnell, N. W., Bertrand, N., Best, M., Folwell, S., Gerten, D., Gomes, S., Gosling, S. N., Hagemann, S., Hanasaki, N., Harding,





HESSD
11, 5559–5597, 2014

R., Heinke, J., Kabat, R., Koirala, S., Oki, T., Polcher, J., Stacke, T., Viterbo, P., Weedon, G. P., and Yeh, P.: Multimodel Estimate of the Global Terrestrial Water Balance: Setup and First Results, J. Hydrometeorol., 12, 869–884, 2011.

He, Y., Wetterhall, F., Bao, H., Cloke, H., Li, Z., Pappenberger, F., Hu, Y., Manful, D., and Huang, Y.: Ensemble forecasting using TIGGE for the July–September 2008 floods in the Upper Huai catchment: a case study, Atmos. Sci. Lett., 11, 132–138, 2010.

Hersbach, H.: Decomposition of the Continuous Ranked Probability Score for Ensemble Prediction Systems, Weather Forecast., 15, 559–570, 2000.

Kling, H., Fuchs, M., and Paulin, M.: Runoff conditions in the upper Danube basin under an ensemble of climate change scenarios, J. Hydrol., 424–425, 264–277, 2012.

Laiolo, P., Gabellani, S., Rebora, N., Rudari, R., Ferraris, L., Ratto, S., Stevenin, H., and Cauduro, M.: Validation of the Flood-PROOFS probabilistic forecasting system, Hydrol. Process., 28, 3466–3481, 2014.

Leutbecher, M. and Palmer, T. N.: Ensemble forecasting, J. Comput. Phys., 227, 3515–3539, 2008.

Mubareka, S., Maes, J., Lavalle, C., and De Roo, A.: Estimation of water requirements by livestock in Europe, Ecosyst. Serv., 4, 139–145, 2013.

NASA: NASA Earth Observatory, Rains in northern Africa have led to wet conditions in Tunisia, available at: http://earthobservatory.nasa.gov/NaturalHazards/view.php?id=10836 (last access: 12 August 2013) 2003.

Pappenberger, F., Thielen, J., and Del Medico, M.: The impact of weather forecast improvements on large scale hydrology: analysing a decade of forecasts of the European Flood Alert System, Hydrol. Process., 25, 1091–1113, 2011.

Pappenberger, F., Stephens, L., van Andel, S. J., Verkade, J. S., Ramos, M. H., Alfieri, L., Brown, J. D., Zappa, M., Ricciardi, G., Wood, A., Pagano, T., Marty, R., Collischonn, W., Le Lay, M., Brochero, D., Cranston, M., and Meissner, D.: HEPEX – Operational HEPS systems around the globe, available at: http://hepex.irstea.fr/operational-heps-systems-around-the-globe/, 2013.

Portuguese Space Office, M. of S.: The Lisbon Declaration on “GMES and Africa.”, 2007.

Ramos, M.-H., Thielen, J., and Bartholmes, J.: EFAS EPS-based forecasts?: in-depth case studies analyses & statistical evaluation of summer 2005 and spring 2006 flood forecasts, available at: http://hepex.nmpi.net/files/download/workshops/3rd/20070628HEPEX-pm-Ramos.pdf, 27–29 June, Stresa, 3rd HEPEX Workshop, 2007.





HESSD

11, 5559–5597, 2014

Rojas, R., Feyen, L., Bianchi, A., and Dosio, A.: Assessment of future flood hazard in Europe using a large ensemble of bias-corrected regional climate simulations, J. Geophys. Res. Atmos., 117, D17109, doi:10.1029/2012JD017461, 2012.
Roulin, E.: Skill and relative economic value of medium-range hydrological ensemble predictions, Hydrol. Earth Syst. Sci., 11, 725–737, doi:10.5194/hess-11-725-2007, 2007.
Sepulcre-Canto, G., Horion, S., Singleton, A., Carrao, H., and Vogt, J.: Development of a Combined Drought Indicator to detect agricultural drought in Europe, Nat. Hazards Earth Syst. Sci., 12, 3519–3531, doi:10.5194/nhess-12-3519-2012, 2012.
Siebert, S. and Döll, P.: The Global Crop Water Model GCWM): Documentation and first results for irrigated crops (University of Frankfurt (Main)), 2008.
Siebert, S. and Döll, P.: Quantifying blue and green virtual water contents in global crop production as well as potential production losses without irrigation, J. Hydrol., 384, 198–217, 2010.
Simmons, A., Uppala, S., Dee, D., and Kobayashi, S.: ERA-Interim: New ECMWF reanalysis products from 1989 onwards (ECMWF), ECMWF Newsletter, available at: http://www.ecmwf.int/publications/newsletters/pdf/110_rev.pdf, 2007.
Thielen, J., Bogner, K., Pappenberger, F., Kalas, M., del Medico, M., and De Roo, A.: Monthly-, medium-, and short-range flood warning: testing the limits of predictability, Meteorol. Appl., 16, 77–90, 2009a.
Thielen, J., Bartholmes, J., Ramos, M.-H., and de Roo, A.: The European Flood Alert System –Part 1: Concept and development, Hydrol. Earth Syst. Sci., 13, 125–140, doi:10.5194/hess-13-125-2009, 2009b.
Thiemig, V., Pappenberger, F., Thielen, J., Gadain, H., De Roo, A., Bodis, K., Del Medico, M., and Muthusi, F.: Ensemble flood forecasting in Africa: a feasibility study in the Juba-Shabelle river basin, Atmos. Sci. Lett., 11, 123–131, 2010.
Thiemig, V., De Roo, A., and Gadain, H.: Current status on flood forecasting and early warning in Africa, Int. J. River Basin Manag., 9, 63–78, 2011.
Thiemig, V., Rojas, R., Zambrano-Bigiarini, M., and De Roo, A.: Hydrological evaluation of satellite-based rainfall estimates over the Volta and Baro-Akobo Basin, J. Hydrol., 499, 324–338, 2013.
Thirel, G., Martin, E., Mahfouf, J.-F., Massart, S., Ricci, S., and Habets, F.: A past discharges assimilation system for ensemble streamflow forecasts over France – Part 1:

Description and validation of the assimilation system, Hydrol. Earth Syst. Sci., 14, 1623–1637, doi:10.5194/hess-14-1623-2010, 2010a.
Thirel, G., Martin, E., Mahfouf, J.-F., Massart, S., Ricci, S., Regimbeau, F., and Habets, F.: A past discharge assimilation system for ensemble streamflow forecasts over France – Part 2: Impact on the ensemble streamflow forecasts, Hydrol. Earth Syst. Sci., 14, 1639–1653, doi:10.5194/hess-14-1639-2010, 2010b.
Thirel, G., Regimbeau, F., Martin, E., Noilhan, J., and Habets, F.: Short-and medium-range hydrological ensemble forecasts over France, Atmos. Sci. Lett., 11, 72–77, 2010c.
Trambauer, P., Maskey, S., Winsemius, H., Werner, M., and Uhlenbrook, S.: A review of continental scale hydrological models and their suitability for drought forecasting in (sub-Saharan) Africa, Phys. Chem. Earth Parts ABC, 66, 16–26, 2013.
UNCSD Secretariat: Disaster Risk Reduction and Resilience Building, (Rio de Janeiro, Brazil), p. 4, 2012.
United Nations (UN): Report of the World Conference on Disaster Reduction (United Nations), 2005.
Van Der Knijff, J. M., Younis, J., and De Roo, A. P. J.: LISFLOOD: a GIS-based distributed model for river basin scale water balance and flood simulation, Int. J. Geogr. Inf. Sci., 24, 189–212, 2010.
Vos, F., Rodriguez, J., Below, R., and Guha-Sapir, D.: Annual Disaster Statistical Review 2008 The numbers and trends, 46, 2009.
Wu, H., Kimball, J. S., Mantua, N., and Stanford, J.: Automated upscaling of river networks for macroscale hydrological modeling, Water Resour. Res., 47, W03517, doi:10.1029/2009WR008871, 2011.
Zambrano-Bigiarini, M. and Rojas, R.: hydroPSO: Model-Independent Particle Swarm Optimisation for Environmental Models (Ispra), 2012.
Zambrano-Bigiarini, M. and Rojas, R.: A model-independent Particle Swarm Optimisation software for model calibration, Environ. Model. Softw., 43, 5–25, 2013.

**Table 1.** Forecast Centres with operational or pre-operational HEPS (http://hepex.irstea.fr/operational-heps-systems-around-the-globe/#comment-1766).

| Forecast centre name | Provider | Domain | Reference |
|---|---|---|---|
| European Flood Awareness System (EFAS) | European Commission (Copernicus) | Europe | www.efas.eu |
| Global Flood Awareness System (GloFAS) | European Commission (JRC)/ECMWF | Global | www.efas.eu, Alfieri et al. (2013) |
| Flood-PRObabilistic Operational Forecasting System (FLOOD-PROOFS) | Compagnia Valdostana delle Acque (CVA) S.p.a | Valle d'Aosta (Northern Italy) | Laiolo et al. (2014) |
| Joint Flood Forecasting System | Environment Agency/Met Office | UK | http://www.ffc-environment-agency.metoffice.gov.uk/ |
| Climate Forecast Applications in Bangladesh (CFAB) | Consortium of Bangladeshi and international organizations and institutes | Bangladesh | http://cfab.eas.gatech.edu/cfab/cfab.html |
| EDF-EPS | EDF | France and Rhine | http://www.lthe.fr/PagePerso//chardon/doc/chardon_EGU_2012.pdf |
| Hydrologic Ensemble Forecasting Service (HEFS) | US National Weather Service | United States | |
| Meteorological Model Ensemble River Forecasts (MMEFS) | US National Weather Service | United States | http://www.erh.noaa.gov/mmefs/ |
| Emilia Romagna Warning operational center | Emilia Romagna Regional Agency Prevention and Environment | Emilia Romagna Italy – Po basin (Northern italy) | |
| French Hydro-meteorological Ensemble Prediction System | Meteo France/French Service for Flood Prediction (SCHAPI) | France | Thirel et al. (2010a, b, c) |
| Watershed simulation and forecasting system (WSFS) | Finnish Environment Institute (SYKE) | Finland | http://www.environment.fi/waterforecast, http://www.ymparisto.fi |
| Swedish flood-forecasting system | Swedish Meteorological and Hydrological Institute (SMHI) | Sweden | http://www.smhi.se, Arheimer et al. (2011) |
| Swiss FEWS-HBV, FEWS-PREVAH, FEWS-WaSiM-ETH | Switzerland | Swiss Rivers: Rhine up to Basel, Linth and Sihl, the Emme, the Rhone. | http://www.hydrodaten.admin.ch/en/index.html#vorhersagen |
| WSL Flood Forecasting | WSL | Sihl, Ticino, Linth and Thur | http://hydro.slf.ch/sihl/chysghl/ |
| 3Tier | 3Tier | Various | http://www.3tier.com/en/package_detail/powersight-basin-monitor-forecasting/ |
| BoM | BoM | Australia | http://www.bom.gov.au/water/ssf/index.shtml |
| Scottish Flood Forecasting Service | SEPA and Met Office | Scotland | http://www.floodforecastingservice.net/ |

**Table 2.** LISFLOOD calibration parameters, including upper and lower bound.

| Parameter | Description | Unit | Min | Max |
|---|---|---|---|---|
| UZTC | Time constant for water in upper zone | days | 5 | 40 |
| LZTC | Time constant for water in lower zone | days | 50 | 2500 |
| GwPV | Groundwater percolation value | $\text{mm day}^{-1}$ | 0.5 | 2 |
| GwLoss | Maximum loss rate out of Lower response box, expressed as a fraction of lower zone outflow | – | 0.01 | 0.7 |
| b_Xinan | Power in Xinanjiang distribution function | – | 0.01 | 1 |
| PPrefFlow | Power that controls increase of proportion of preferential flow with increased soil moisture storage | – | 1 | 4 |
| CCM | Multiplier applied to Channel Manning's n | – | 0.1 | 15 |
| TransSub | transmission loss function parameter | – | 0 | 0.6 |
| rnlim | normal reservoir storage limit (fraction) | – | 0.1* | 0.9* |
| rflim | food reservoir storage limit (fraction) | – | 0.7* | 1.0* |
| rnormq | non damaging reservoir outflow | $m^3 s^{-1}$ | 0.1* | 2000* |
| rndq | normal outflow | $m^3 s^{-1}$ | 12* | 3000* |

* Ranges are reservoir dependent.



Discussion Paper | Discussion Paper | Discussion Paper | Discussion Paper |

HESSD

11, 5559–5597, 2014

A pan-african flood forecasting system

V. Thiemig et al.

HESSD
11, 5559–5597, 2014

A pan-african flood forecasting system

V. Thiemig et al.





**Table 3.** Contingency table for flood events.

| | | observed | |
|---|---|---|---|
| | | yes | no |
| forecasted | yes | hits (H) | false alarms (FA) |
| | no | misses (M) | correct negatives (CN) |

**Table 4.** Semi-qualitative evaluation of AFFS ability to detect flood events.

| | | hits | false alarms | misses | POD [%] | FAR [%] | CSI [%] |
|---|---|---|---|---|---|---|---|
| general | | 27 | 11 | 12 | 69 | 29 | 54 |
| different regions | Northern Africa | 3 | 1 | 2 | 60 | 25 | 50 |
| | Western Africa | 6 | 0 | 4 | 60 | 0 | 60 |
| | Eastern Africa | 9 | 4 | 2 | 82 | 31 | 60 |
| | Southern Africa | 9 | 4 | 4 | 69 | 31 | 53 |
| flood duration | ≤ 1 week | 8 | 1 | 7 | 53 | 11 | 50 |
| | > 1 week | 19 | 10 | 5 | 79 | 34 | 56 |
| average amount of annual precipitation | ≤ 600 mm | 11 | 3 | 3 | 79 | 21 | 65 |
| | > 600 mm | 16 | 5 | 9 | 64 | 24 | 53 |
| affected area | ≤ 10 000 $km^2$ | 15 | 1 | 10 | 60 | 6 | 58 |
| | > 10 000 $km^2$ | 12 | 8 | 2 | 86 | 40 | 55 |
| mean annual discharge (in affected area) | ≤ 10 $km^2\ year^{-1}$ | 12 | 7 | 7 | 63 | 37 | 46 |
| | > 10 $km^2\ year^{-1}$ | 15 | 4 | 5 | 75 | 21 | 63 |



HESSD
11, 5559–5597, 2014



Discussion Paper | Discussion Paper | Discussion Paper | Discussion Paper |
Title Page
Abstract Introduction
Conclusions References
Tables Figures
◂◂ ▸▸
◂ ▸
Back Close
Full Screen / Esc
Printer-friendly Version
Interactive Discussion

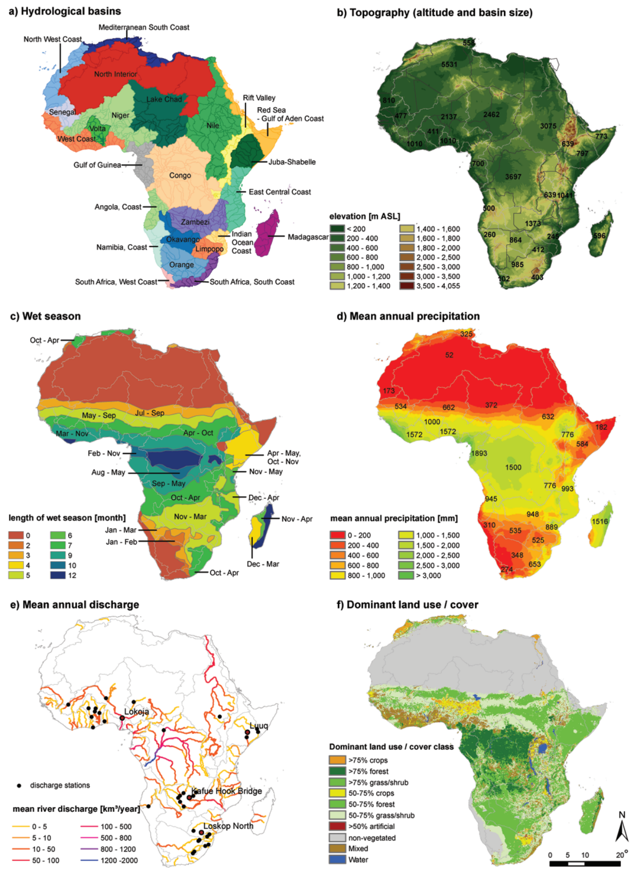


**Figure 1.** Overview of the study area; including **(a)** delineation of the hydrological basins (FAO), **(b)** altitude [m a.s.l.] and river basin size [1000 km$^2$], **(c)** time period and length of the wet season (derived from CRU), **(d)** mean annual precipitation [mm] (CRU), **(e)** mean annual river discharge [km$^3$] (GRDC) and discharge station network and **(f)** dominant land use/cover (USGS).





HESSD
11, 5559–5597, 2014

A pan-african flood forecasting system

V. Thiemig et al.

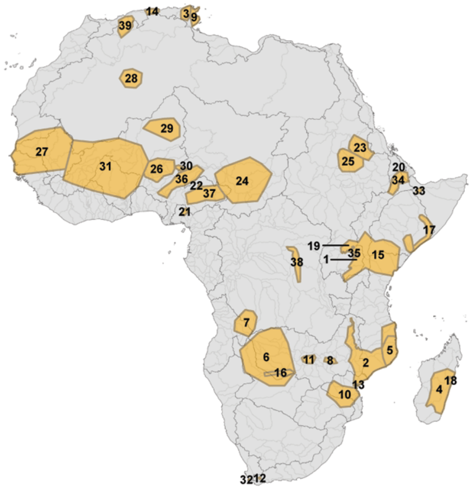


| ID | time period | countries | river (or region / city) | 1* | 2* | 3* | 4* |
|---|---|---|---|---|---|---|---|
| 1 | 04 - 06 Jan | Kenya | Auji | x | x | | |
| 2 | 01 – 17 Jan | Malawi, Mozambique | Lower Zambezi, Shire, (coast of Mozambique) | x | x | x | x |
| 3 | 14 – 16 Jan | Tunisia | Oued Mejerda | x | x | x | x |
| 4 | 18 – 31 Jan | Madagascar | Ikopa | x | x | x | x |
| 5 | 04 – 17 Feb | Mozambique | Pemba-Metuge District | x | x | | |
| 6 | 15 Jan – 01 Jul | Zambia, Angola, Namibia | Upper Zambezi and tributaries | x | x | x | |
| 7 | 06 – 20 Feb | Angola | Upper Cuanza, Cuanango | x | | | |
| 8 | 25 – 28 Feb | Zimbabwe | Musengezi, Manyane (influences to Cahora Bassa) | x | x | | |
| 9 | Feb | Tunesia | - | | | x | |
| 10 | 05 – 18 Mar | Mozambique; Zimbabwe | Save and tributaries | x | | | |
| 11 | 11 – 15 Mar | Zambia | Kafue | x | x | | |
| 12 | 23 – 26 Mar | South Africa | Kigna, Keisie | x | x | | |
| 13 | 26 – 28 Mar | Mozambique | Pungwe | x | x | | |
| 14 | 02 - 05 Apr | Algeria | Oued Sebaou | | x | | |
| 15 | 21 Apr – 04 Jun | Kenya, Uganda | Tana, Lag Dere | x | x | | x |
| 16 | Apr - May | Namiba | Cuando/ Chobe (Caprivi Stripe) | | | x | x |
| 17 | 05 Apr – 20 May | Somalia, Ethiopia | Juba-Shabelle | x | x | x | |
| 18 | 08 – 12 May | Madagascar | (Toamasina town) | x | | | |
| 19 | 01 – 03 Jul | Uganda | Manafwa | x | x | | |
| 20 | 19 Jul – 01 Aug | Ethiopia | Awash | x | | | |
| 21 | 23 – 25 Jul | Nigeria | Cross | x | | | |
| 22 | 22 – 24 Jul | Nigeria | Gongola | x | | | |
| 23 | 28 Jul – 21 Aug | Sudan, Eritrea | Gash, Atbara, Siteet | x | x | x | x |
| 24 | 03 Aug – 02 Nov | Chad, Central African Republic | Chari, Logone | x | | | |
| 25 | 03 – 25 Aug | Sudan | White Nile, Blue Nile | x | | x | |
| 26 | 05 Aug – 12 Oct | Nigeria | Sokoto, main Niger | x | | | |
| 27 | 09 Aug – 05 Nov | Senegal, Gambia, Guinea-Bissau, Mauritania | Senegal, Gambia, Geba (all incl. tributaries) | x | x | x | x |
| 28 | 09 – 11 Aug | Algeria | Reggane (Adrar region) | x | x | | |
| 29 | Aug | Algeria, Niger | Ti-n-Amzi, Irhazer Oua-n-Agade | | x | | |
| 30 | 08 – 24 Aug | Nigeria | Hadejia | x | | | |
| 31 | 18 – 21 Aug | South Africa | Breeriver (Montagu area) | x | | | |
| 32 | 10 Aug – 19 Oct | Burkina Faso; Mali | Niger and tributaries; White and Black Volta; Ot | x | x | | |
| 33 | 18 – 20 Aug | Somalia | Hargeisa | x | x | | |
| 34 | 19 Aug – 09 Sep | Ethiopia | Awash | x | | x | |
| 35 | 26 Aug – 12 Sep | Kenya | Nzoia, Yala | x | | | |
| 36 | 05 Sep – 28 Oct | Nigeria | Lower Niger; Hadejia and Jamaare | x | x | | x |
| 37 | 22 Sep – 10 Oct | Nigeria | Benue | x | | | |
| 38 | Oct | Democratic Republic of the Congo | Middle Congo (Kisangani) | | x | | |
| 39 | 15 – 18 Oct | Algeria | - | x | x | | |

* reported by 1 = Dartmouth Flood Observatory; 2 = Emergency Events Database EM-DAT; 3 = NASA Earth Observatory; 4 = reliefweb

**Figure 2.** Flood events in Africa, in 2003, as reported by various disaster databases (Dartmouth Flood Observatory, Emergency Events Database EM-DAT, NASA Earth Observatory and Reliefweb). Map on left indicates the outline of the affected regions, while table on right gives further details on time period and location.



HESSD
11, 5559–5597, 2014

A pan-african flood forecasting system

V. Thiemig et al.

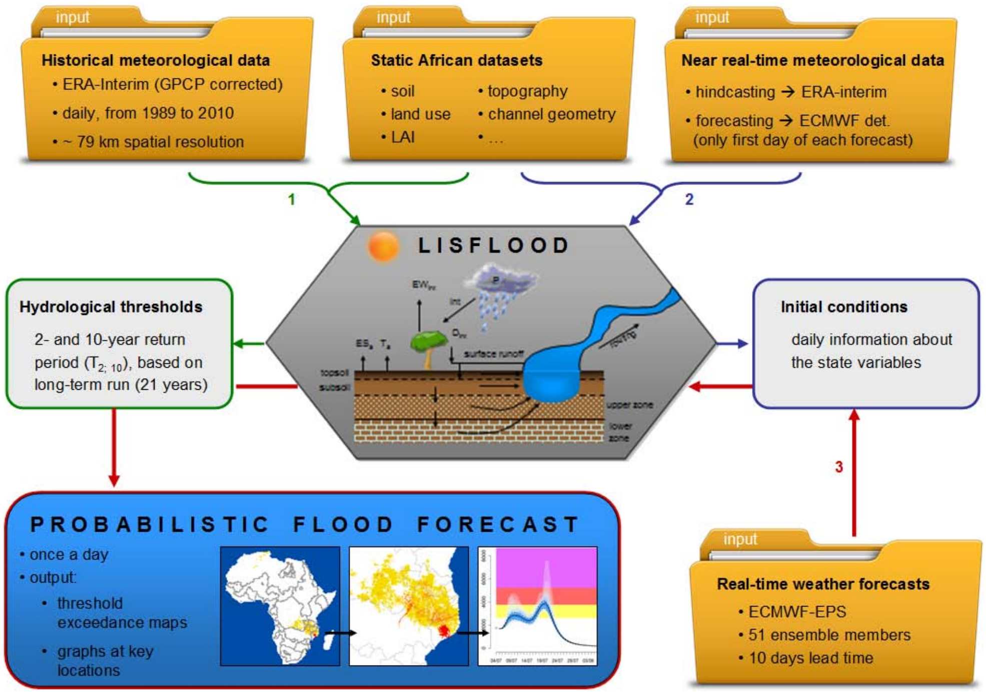


**Figure 3.** Schematic overview of AFFS.





HESSD
11, 5559–5597, 2014

HESSD
11, 5559–5597, 2014





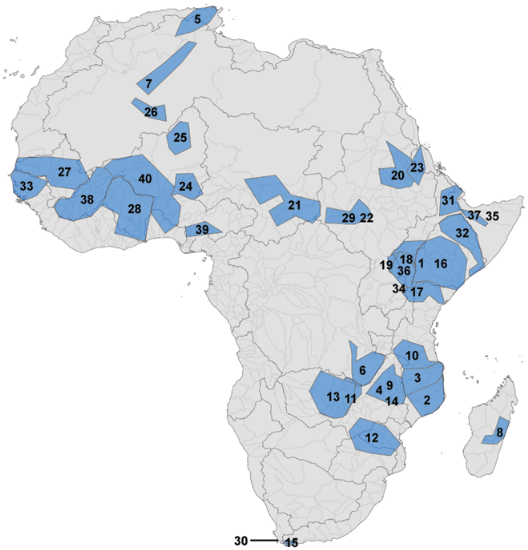


| AFFS-ID | time period | countries | river (or region) | obs-ID |
|---|---|---|---|---|
| 1 | 02 - 06 Jan | Kenya | - | 1 |
| 2 | 05 Jan - 07 Apr | Mozambique | (Nampula and Cabo Delgado districts) | 2, 5 |
| 3 | 08 Jan - 18 Apr | Mozambique | Ruvuma | 2 |
| 4 | 12 - 21 Jan | Mozambique, Zambia, Malawi | Lower Zambezi | 2 |
| 5 | 12 Jan - 12 Feb | Tunesia | Oued Mejerda | 3, 9 |
| 6 | 15 Jan - 28 Apr | Zambia | Chambeschi | - |
| 7 | 17 - 23 Jan | Algeria | - | - |
| 8 | 17 - 19 Jan | Madagascar | Ikopa | 4 |
| 9 | 11 - 25 Feb | Mozambique, Zambia, Malawi | Lower Zambezi | - |
| 10 | 13 - 26 Feb | Tanzania | (Lindi district) | - |
| 11 | 12 Feb - 16 Mar | Zambia | Kafue | 11 |
| 12 | 03 - 15 Mar | Mozambique | Save and tributaries | 10 |
| 13 | 1 Mar - 30 Apr | Zambia | Upper Zambezi, Kafue | 6, 16 |
| 14 | 27 Mar - 15 Apr | Zambia, Malawi | Luangwa, Shire | - |
| 15 | 23 - 26 Mar | South Africa | Kigna, Keisie | 12 |
| 16 | 19 Apr - 31 May | Ethiopia, Somalia, Kenya | Juba, Lag Dere | 15, 17 |
| 17 | 26 Apr - 24 May | Kenya | Tana | 15 |
| 18 | 29 Apr - 31 May | Kenya, Ethiopia | Lake Turkana | - |
| 19 | 01 Jul - 21 Sep | border Uganda/ Kenya | - | 19 |
| 20 | 31 Jul - 13 Sep | Sudan | White Nile, Blue Nile | 25 |
| 21 | 04 Aug - 12 Sep | Chad, Central Republic of Africa | tributaries of Chari | 24 |
| 22 | 05 - 13 Aug | Sudan | Lol, Bahr el'Arab | - |
| 23 | 07 - 13 Aug | Sudan, Eritrea | Gash, Atbara, Siteet | 23 |
| 24 | 07 - 27 Aug | Nigeria | Sokoto, Hadejia | 26 |
| 25 | 09 - 22 Aug | Algeria, Niger | Ti-n-Amzi, Irhazer Oua-n-Agade | 29 |
| 26 | 10 - 15 Aug | Algeria | Reggane (Adrar region) | 28 |
| 27 | 10 Aug - 26 Sep | Mauritania, Mali | Senegal | 27 |
| 28 | 11 Aug - 09 Oct | Burkina Faso, Ghana | Volta | 32 |
| 29 | 13 Aug - 10 Sep | Sudan | Lol, Bahr el'Arab | - |
| 30 | 17 - 19 Aug | South Africa | Breeriver (Montagu area | 31 |
| 31 | 18 - 21 Aug | Ethiopia, Sudan | Awash | 34 |
| 32 | 18 Aug - 23 Sep | Ethiopia, Somalia | Shabelle | - |
| 33 | 18 Aug - 03 Nov | Senegal, Gambia, Guinea-Bissau | Gambia, Geba | 27 |
| 34 | 19 Aug - 22 Sep | Kenya | Turkwel, Kerio | - |
| 35 | 19 Aug - 03 Sep | Somalia | Hargeisa, Nugaal | 33 |
| 36 | 24 Aug - 17 Sep | Kenya | Nzoia, Yala | 35 |
| 37 | 13 - 24 Sep | Somalia | Hargeisa | - |
| 38 | 03 Sep - 31 Oct | Mali | Upper Niger and tributaries | 32 |
| 39 | 22 Sep - 04 Oct | Nigeria | Benue | 37 |
| 40 | 04 Oct - 05 Dec | Mali, Niger, Nigeria | Middle and Lower Niger | 26 |

**Figure 4.** Flood events in Africa, in 2003, as forecasted by AFFS. Map on left indicates the outline of the affected regions, while table on right gives further details on time period and location.

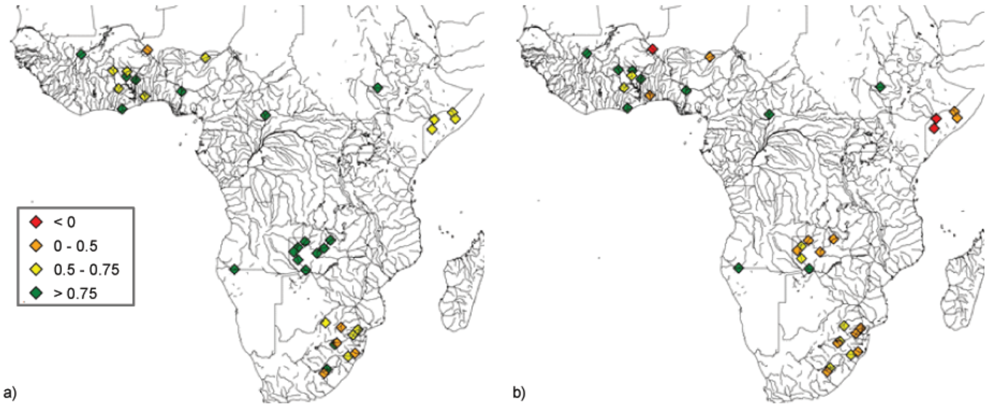


**Figure 5.** Modified Kling-Gupta efficiencies between daily LISFLOOD simulated and observed discharge for **(a)** the calibration period 2004–2008 and **(b)** the validation period 1998–2003.



HESSD
11, 5559–5597, 2014

A pan-african flood forecasting system

V. Thiemig et al.

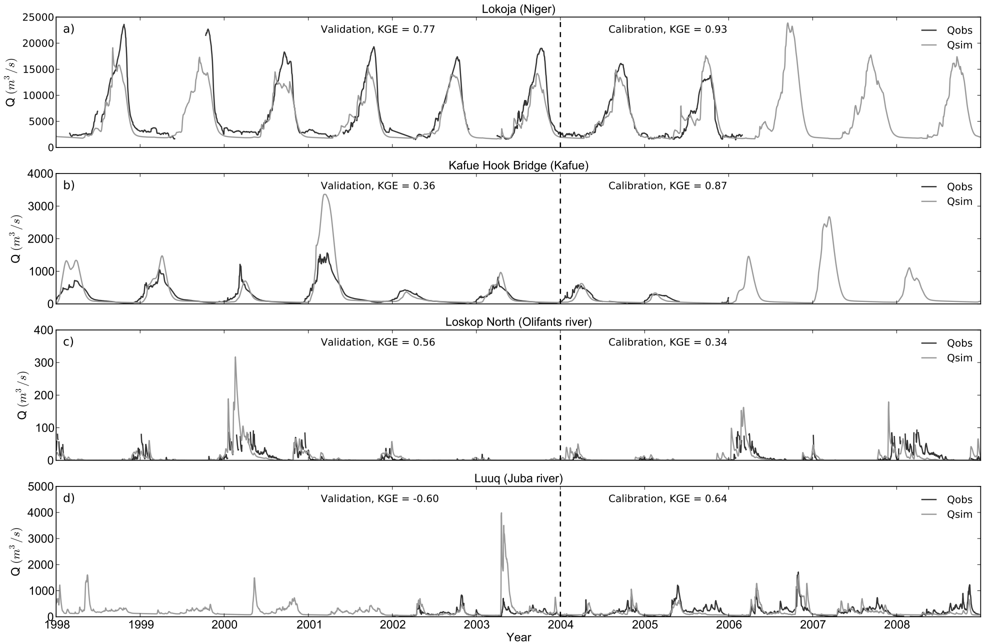


**Figure 6.** Comparison of daily LISFLOOD simulated (Qsim) and observed (Qobs) hydrographs during both the validation (1998–2003) and calibration period (2004–2008), for **(a)** Niger River at Lokoja (2 174 000 km$^2$), **(b)** Kafue River at Kafue Hook Bridge (100 000 km$^2$), **(c)** Olifants River at Loskop North (15 000 km$^2$), and **(d)** Juba River at Luuq (169 000 km$^2$).





HESSD
11, 5559–5597, 2014

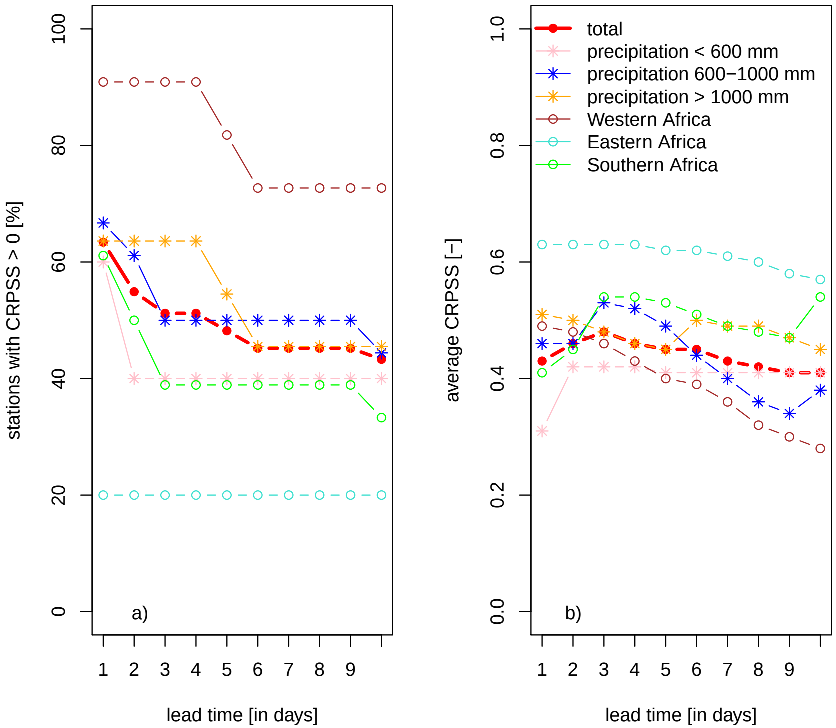


**Figure 7.** Continuous Rank Probability Skill Score over the 10 day lead time; **(a)** amount of stations with CRPSS > 0 and **(b)** average CRPSS (only within the limit of predictability).

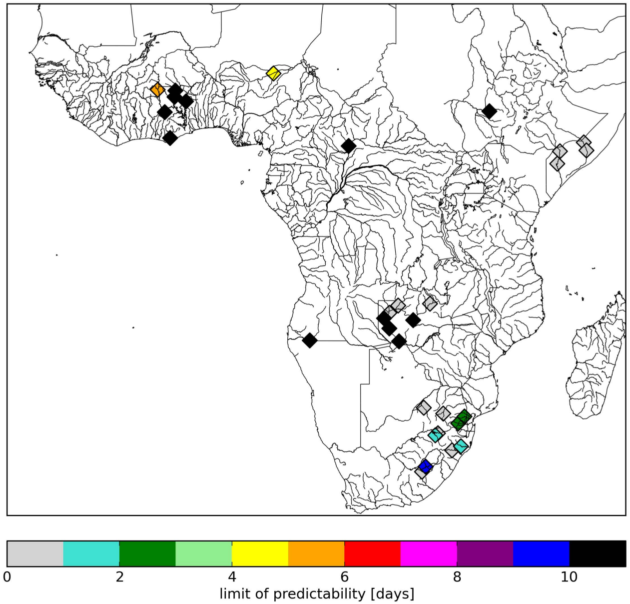


**Figure 8.** Limit of predictability at the selective stations.





HESSD
11, 5559–5597, 2014

A pan-african flood forecasting system

V. Thiemig et al.

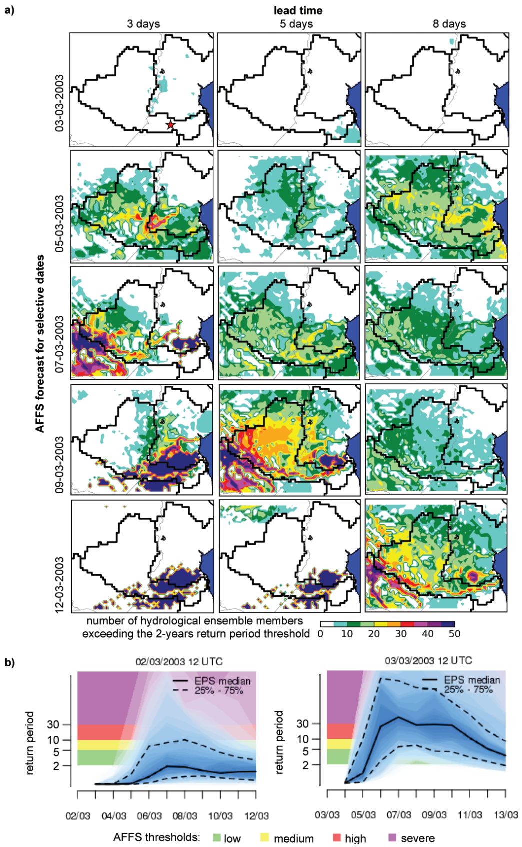


**Figure 9.** AFFS forecast of the March flooding in the Save Basin (102 000 $km^2$); **(a)** shows the threshold exceedance maps for a number of selective forecasted days and lead times; while the ensemble quantiles plot in **(b)** show the temporal development of the AFFS forecast for a specific key location (for the location see red star in upper left panel of **(a)**).



HESSD
11, 5559–5597, 2014

A pan-african flood forecasting system

V. Thiemig et al.

Title Page
Abstract | Introduction
Conclusions | References
Tables | Figures
◀| |▶
◀ ▶
Back | Close
Full Screen / Esc
Printer-friendly Version
Interactive Discussion